



ELSEVIER

Journal of Luminescence 96 (2002) 269–278

JOURNAL OF
LUMINESCENCE

www.elsevier.com/locate/jlumin

Electronic energy transfer in polymers labeled at both ends with fluorescent groups

E.N. Bodunov, M.N. Berberan-Santos, J.M.G. Martinho*

Centro de Química-Física Molecular, Instituto Superior Técnico, Complexo I, Av. Rovisco Pais, 1, 1049-001 Lisboa, Portugal

Received 30 January 2001; received in revised form 13 June 2001; accepted 13 June 2001

Abstract

The energy transfer between chromophores attached at the ends of an isolated polymer chain was studied. Chains labeled with different or equal fluorophores at the ends were considered. Interpolated analytical expressions dependent on a unique parameter, were derived for the fluorescence decay curves taking into account the distribution of end-to-end separations in both θ and good solvents for the polymer. The donor decay curves for chains with dissimilar chromophores were compared with the exact solution obtained by numerical integration. The derived expressions reproduce the decay for all times with a precision better than 1% for pseudo-ideal chains (θ solvents) and 3% for chains in good solvents. The inhomogeneous broadening of chromophore spectra is important when its width is larger than 20% of the homogeneous broadening width.

The fluorescence decay curves in the presence of Brownian motion were also calculated after solving the Smoluchowski diffusion equation for the end-to-end separation distance distribution function. Chain dynamics is important for donors with long lifetimes, high diffusion coefficients and donor–acceptor pairs with small Förster radius.

© 2002 Elsevier Science B.V. All rights reserved.

Keywords: Polymers; Fluorescence; Electronic energy transfer; Inhomogeneous broadening

1. Introduction

The fluorescence of polymers has been used to extract relevant structural and dynamic information on polymer systems, both in solution and in the bulk. Particularly useful is the study of the energy transfer between similar or different fluorophores attached to the polymer chain [1,2]. In general, the energy transfer occurs by both short and long range interactions, but the long range dipole–dipole term is usually dominant [3]. The

energy transfer rate by a dipole–dipole coupling mechanism has a $1/r^6$ dependence on the donor–acceptor separation and so the fluorescence decay curves strongly reflect the distribution of distances between the chromophores, providing relevant information on the conformation and dynamics of polymers. For moderate polymer densities, the fluorescence observables become very complex due to the intermolecular energy transfer processes [1,4]. For this reason, the experiments are generally performed under very dilute conditions, allowing intermolecular excitation transfer to be neglected.

Three different types of chromophore attachment to a linear polymer chain can be

*Corresponding author. Tel.: +351-21-8419250; fax: +351-21-846-4455.

E-mail address: jgmartinho@ist.utl.pt (J.M.G. Martinho).

considered: The simplest case consists of polymers with simply one donor and one trap chromophores [5,6]. Fluorescent tagged polymers synthesized from macromolecules with functional groups of much different reactivity towards the donor and traps and some biomolecules belong to this category. The second case consists of donor and trap chromophores randomly distributed among the sites of each polymer chain [1,4,6–11]. The occupancy of a particular site is independent of the type and number of chromophores substituted at other sites. Such polymers can be synthesized by esterification of long chain dialcohols with acids (containing a donor or a trap) that have equal reactivity towards the alcohol. The third and last case consists of polymers with a regular distribution of donor chromophores along the chains, while the acceptor distribution is random [1,2,12–14]. The aromatic vinyl polymers with very low concentration of excimer forming sites (traps) belong to this group.

The aim of this work is to study the direct incoherent energy transfer from an electronic excited fluorophore at one polymer chain end to a similar or different molecule at the opposite end. Interchain transfer events are neglected, which supposes the use of very dilute solutions. It was also assumed that the polymer adopts a coil conformation with known end-to-end distance distribution function for both θ and good solvents and that the energy transfer occurs by a dipole–dipole coupling mechanism. First, the influence of the end-to-end chain distance distribution function was studied, considering an immobile chain during the energy transfer events (static transfer). Next, chain dynamics is introduced using a Smoluchowski diffusion equation for the chain end-to-end distance distribution function of a harmonic spring chain (dynamic transfer).

2. Static energy transfer

2.1. Donor-to-acceptor energy transfer

The energy transfer rate between a donor and an acceptor separated by a distance r , and considering only the dipole–dipole interaction

term, is given by

$$w(r) = \frac{1}{\tau} \left(\frac{R_0}{r} \right)^6, \quad (1)$$

where R_0 is the Förster radius and τ the fluorescence lifetime of a donor in the absence of acceptors. For a polymer chain with a donor at one end and an acceptor at the other one and neglecting the back transfer, the number density of donor excited molecules obeys the rate equation

$$\frac{d}{dt} p(r, t) = -w(r)p(r, t). \quad (2)$$

The intrinsic processes of deactivation of the donor are not considered because they are independent of the transfer events and can be included by multiplication of the final expressions by the intrinsic donor decay, $\exp(-t/\tau)$. For a constant chain end-to-end distance, the integration of Eq. (2) gives

$$p(r, t) = p(r, 0) \times \exp[-tw(r)], \quad (3)$$

where $p(r, 0)$ is the initial density of donor excited molecules. However, as the polymer is polydisperse and several conformation chains with different end-to-end distances exist in solution, Eq. (3) should be averaged. Considering a monodisperse polymer with N statistical segments and end-to-end distance distribution function, $g_N(r)$, the averaged excited donor density, for $p(r, 0) = 1.0$, is

$$p(t) = 4\pi \int_0^\infty r^2 g_N(r) e^{-tw(r)} dr. \quad (4)$$

The conformation of a polymer in solution varies with temperature. At the θ temperature the attraction and repulsion between polymer segments cancel out, the second virial coefficient vanishes and the behavior of the polymer becomes ideal. The solvent at this temperature is named a θ solvent for the polymer, and the end-to-end distance distribution function is given by [5,15]

$$g_N(r) = A_1 \exp(-B_1 r^2) \quad (5)$$

with

$$A_1 = \left(\frac{3}{2\pi \langle R_N^2 \rangle} \right)^{3/2}; \quad B_1 = \frac{3}{2 \langle R_N^2 \rangle}. \quad (6)$$

In a good solvent the chain is expanded due to the dominance of the polymer segment–segment repulsion (exclude volume effects), being the chain conformation described by a self-avoiding walk (SAW) in a lattice. The distribution function is no more Gaussian, being then

$$g_N(r) = A_2 r^{5/18} \exp(-B_2 r^{5/2}) \tag{7}$$

with

$$A_2 = 0.289058 / \langle R_N^2 \rangle^{59/36};$$

$$B_2 = 1.22271 / \langle R_N^2 \rangle^{5/4}, \tag{8}$$

where $\langle R_N^2 \rangle$ is the average square end-to-end distance ($\langle R_N^2 \rangle = Nl^2$ for a pseudo-ideal chain and $\langle R_N^2 \rangle = N^{6/5}l^2$ for a SAW chain), l is the statistical segment length (Kuhn length).

Fig. 1 shows the distribution function, $g_N(r)$ versus the reduced distance $x = r / \sqrt{\langle R_N^2 \rangle}$ for both a pseudo-ideal (Eq. (5)) and a SAW chain (Eq. (7)). These distribution functions reproduce well (within 2%) the computer-simulation data and

their accuracy is in general sufficient to describe the conformations of real polymer chains [15].

Inserting Eq. (5) into Eq. (4) and using the new variable of integration $y = \frac{3}{2} r^2 / \langle R_N^2 \rangle$, we obtain for the pseudo-ideal chain

$$p_{id}(t) = \frac{2}{\pi^{1/2}} \int_0^\infty y^{1/2} \exp\left(-y - \frac{27T}{8y^3}\right) dy \tag{9}$$

with

$$T = \frac{R_0^6}{\langle R_N^2 \rangle^3} \frac{t}{\tau}. \tag{10}$$

Eq. (9) depends on a single parameter, T . The integral was evaluated by the method of steepest descendent [5] and the asymptote for long times, ($t/\tau \gg 1$), obtained as

$$p_{id}(t \rightarrow \infty) \propto T^{1/4} \exp(-2^{5/4} T^{1/4}). \tag{11}$$

Taking into account this asymptotic form and the decay limits of Eq. (9) for initial and long times, the interpolation equation

$$p_{id}(t) = (1 + bT^{1/4}) \exp(-2^{5/4} T^{1/4}) \tag{12}$$

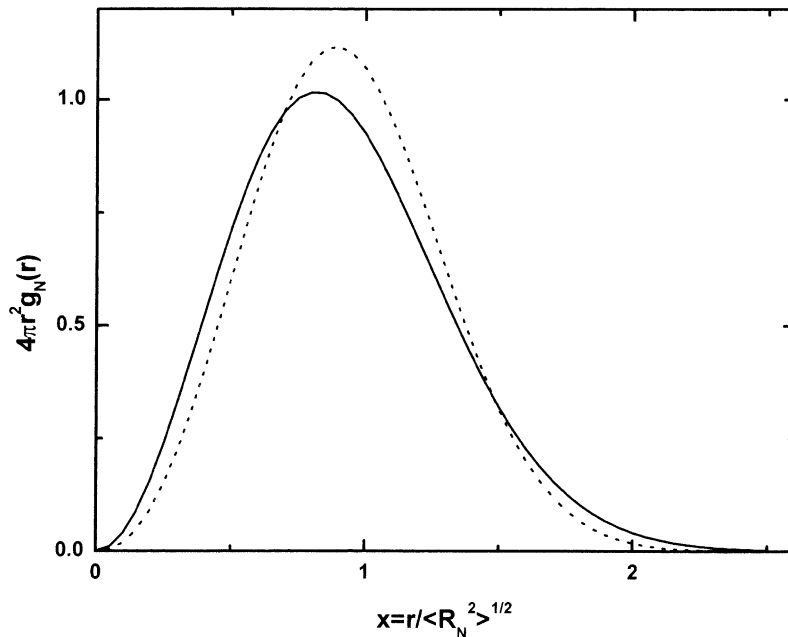


Fig. 1. Plot of the end-to-end separation distribution functions for an ideal (—) and a SAW (.....) polymer chains versus $x = r / \sqrt{\langle R_N^2 \rangle}$.

was used in a linear least-squares fit to the numerical values to calculate the best value of b . The best value of b was 2.45. Therefore, an approximate decay law that replaces Eq. (9) is

$$p_{id}(t) = (1 + 2.45T^{1/4})\exp(-2^{5/4}T^{1/4}). \quad (13)$$

This equation describes well the decay for all times with a precision better than 1%.

For a chain with excluded volume interactions (SAW chain),

$$p_{SAW}(t) = \frac{1}{\Gamma(1 + 14/45)} \times \int_0^\infty y^{14/45} \exp\left[-y - \left(\frac{\Gamma(19/9)}{\Gamma(59/45)}\right)^3 \frac{T}{y^{12/5}}\right] dy, \quad (14)$$

where $y = B_2 r^{5/2}$. Working similarly as for the case of the Gaussian chain, the interpolation formula

$$p_{SAW}(t) = (1 + 1.75T^{73/306})\exp(-2.1122T^{5/17}) \quad (15)$$

was obtained. Eqs. (13) and (15), after being multiplied by $\exp(-t/\tau)$, can be used to fit the experimental decays. These analytical expressions

have great advantages over the integral Eqs. (9) and (14), because the calculation of the integral is avoided in each step of the fitting procedure to the experimental decays. In the past both numerical integration [6] and its asymptotic forms for long times ($t/\tau \gg 1$) [5] were used. By fitting the experimental donor decays, it is possible to recover $\langle R_N^2 \rangle$ and predict the quality of the solvent to the polymer. However, the solution of this problem is not trivial, because the shape of the decay predicted by Eqs. (13) and (15) is identical (see Fig. 2). A better discrimination procedure can be envisaged if polymer chains of several molecular weights are studied. In this case the power law dependence of $\sqrt{\langle R_N^2 \rangle}$ with the degree of polymerization gives a different exponents for θ solvents (0.5) and good solvents (0.6).

2.2. Donor-to-donor transfer

We will consider now the case of a chain both ends labeled with the same fluorophore. The decay of the donor is described by the following

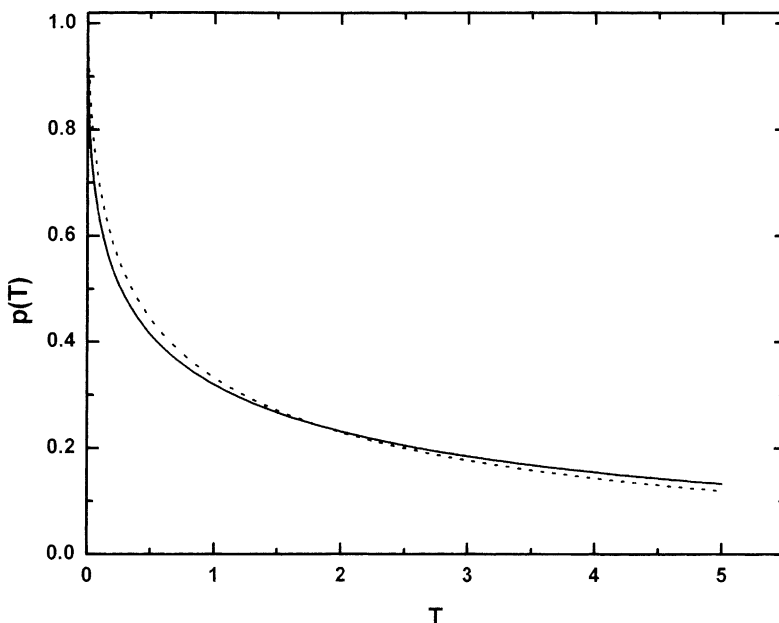


Fig. 2. Fluorescence donor decay, $p(T)$ for pseudo-ideal (—) and a SAW (.....) polymer chains versus $T = \left(R_0^6 / \langle R_N^2 \rangle^3\right) t/\tau$, from Eqs. (9) and (14), respectively.

equations:

$$\frac{d}{dt}p_1(r, t) = -w(r)[p_1(r, t) - p_2(r, t)], \quad (16a)$$

$$\frac{d}{dt}p_2(r, t) = w(r)[p_1(r, t) - p_2(r, t)]. \quad (16b)$$

The solution to these equations, assuming that the donor 1 is excited at time zero, $p(r, 0) = 1.0$, is

$$p_1(r, t) = \frac{1}{2} + \frac{1}{2}\exp[-2tw(r)]. \quad (17)$$

The ensemble-average probability that an originally excited molecule is still excited at time t , $G^s(t)$, is obtained by averaging Eq. (17) with the distribution function $g_N(r)$. $G^s(t)$ contains contributions from the original excited molecules and from re-excitations after one or more transfer events. Proceeding in a similar way as before, the interpolation formulas for the pseudo-ideal chain (precision > 1%)

$$G_{id}^s(t) = \frac{1}{2} + \frac{1}{2}(1 + 2.45T_1^{1/4})\exp(-2^{5/4}T_1^{1/4}) \quad (18)$$

and for the SAW chain (precision > 3%)

$$G_{SAW}^s(t) = \frac{1}{2} + \frac{1}{2}(1 + 1.75T_1^{73/306}) \times \exp(-2.1122T_1^{5/17}) \quad (19)$$

were obtained, with

$$T_1 = 2T = \frac{2R_0^6}{\langle R_N^2 \rangle^3} \frac{t}{\tau}. \quad (20)$$

The anisotropy of fluorescence $r(t)$ and $G^s(t)$ are related by

$$r(t) = r_0G^s(t), \quad (21)$$

where r_0 is the anisotropy at the initial time [4,11,16]. Fig. 3 compares the values of $G^s(t)$ calculated by Eqs. (18) and (19). As expected $G^s(t) \rightarrow 1/2$ at long times, because each chain contains exactly two donors and the excitation has equal probability of being in each one at infinity time, since no intrinsic deactivation processes were considered.

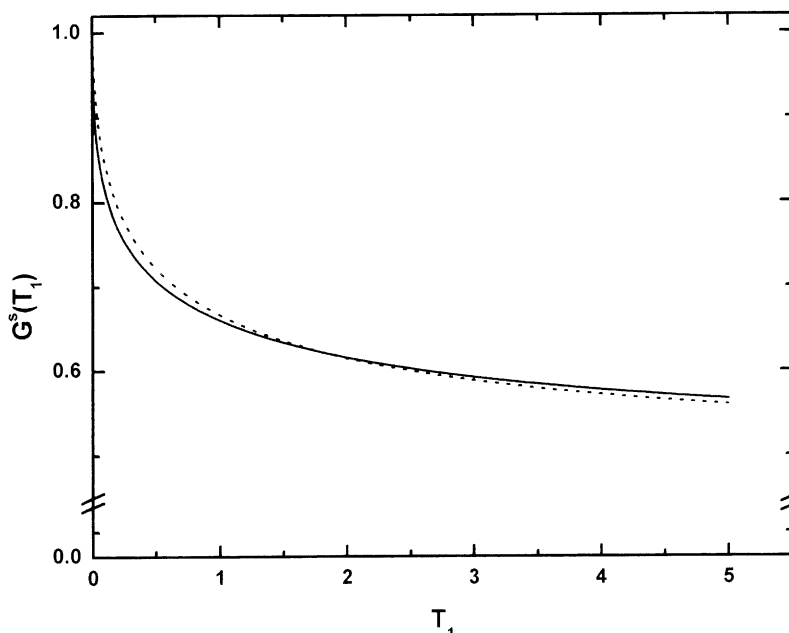


Fig. 3. Ensemble average probability $G^s(T)$, that an originally excited chromophore remains excited at time t , versus $T = (R_0^6 / \langle R_N^2 \rangle^3) t / \tau$, for a pseudo-ideal ideal (—) and a SAW (....) polymer chain, calculated from Eqs. (18) and (19), respectively.

2.3. Inhomogeneous broadening

In recent years special attention has been paid to polymer containing donor and acceptor chromophores with inhomogeneous spectral broadening [2]. In these polymers the fluorescence decays, at a given temperature, are influenced by both the excitation wavelength and pulse spectral width. In the case of inhomogeneous spectral broadening, the donor decay curve (under non-selective excitation), can be written as

$$p_{\text{inh}}(t) = \int g_{\text{D}}(E_1) dE_1 \int g_{\text{A}}(E_2) dE_2 \times \int dr 4\pi g_{\text{N}}(r) e^{-tw(E_1 - E_2, r)}, \quad (22)$$

where $w(E_1 - E_2, r)$ is the rate of energy transfer from a donor to an acceptor having transition energies E_1 and E_2 , and $g_{\text{D}}(E_1)$ and $g_{\text{A}}(E_2)$ are the normalized distributions of donor and acceptor chromophores over transition energies. For simplicity, we will consider Gaussian distributions with equal widths, σ , and maximums located at the transition energies E_{D} and E_{A} ,

$$g_{\text{D}}(E) = \frac{1}{\sqrt{2\pi}\sigma} \exp\left[-\frac{(E_{\text{D}} - E)^2}{2\sigma^2}\right] \quad (23a)$$

$$g_{\text{A}}(E) = \frac{1}{\sqrt{2\pi}\sigma} \exp\left[-\frac{(E_{\text{A}} - E)^2}{2\sigma^2}\right] \quad (23b)$$

and that the homogeneous spectra of emission of donors and absorption of acceptors have also a Gaussian shape of width, $\delta/\sqrt{2}$. The rate of energy transfer by dipole–dipole mechanism (being proportional to the overlap integral of the spectra [3]) can be written as

$$w(E_1 - E_2, r) = \frac{1}{\tau} \left[\frac{R(E_1 - E_2)}{r} \right]^6 \quad (24)$$

with

$$R^6(E_1 - E_2) = R_0^6 \exp\left[-\frac{(E_1 - E_2)^2}{\delta^2} + \left(\frac{E_{\text{D}} - E_{\text{A}}}{\delta}\right)^2\right], \quad (25)$$

where R_0 is the Förster radius of energy transfer from a donor to an acceptor having transition energies $E_1 = E_{\text{A}}$ and $E_2 = E_{\text{D}}$.

The third integral in Eq. (22) was calculated as in Section 2.1. Using this result and substituting Eq. (24) into Eq. (22), we obtain

$$p_{\text{inh}}(t) = \int g_{\text{D}}(E_1) dE_1 \times \int g_{\text{A}}(E_2) dE_2 [1 + 2.45T^{1/4}(E_1 - E_2)] \times \exp[-2^{5/4}T^{1/4}(E_1 - E_2)] \quad (26)$$

with

$$T(E_1 - E_2) = \frac{t}{\tau} \frac{R_0^6}{\langle R_{\text{N}}^2 \rangle^3} \times \exp\left[-\frac{(E_1 - E_2)^2}{\delta^2} + \left(\frac{E_{\text{D}} - E_{\text{A}}}{\delta}\right)^2\right]. \quad (27)$$

Fig. 4 shows the results of the numerical integration of Eq. (26) for $E_{\text{D}} = E_{\text{A}}$. It can be seen that the increase of inhomogeneous broadening (the ratio σ/δ) slows down the emission decay, because the broadening decreases the rate of energy transfer for all donor–acceptor pairs (see Eqs. (24) and (25)).

The donor decays were also calculated for $E_{\text{D}} - E_{\text{A}} = 2\sigma$ and the results are plotted in Fig. 5. In this case the decay is faster at the beginning but at long times become slower, because the rate of energy transfer increases for donor–acceptor pairs with $E_1 - E_2 < E_{\text{D}} - E_{\text{A}}$ and decreases for pairs with $E_1 - E_2 > E_{\text{D}} - E_{\text{A}}$ (see Eqs. (24) and (25)). In any case, the influence of inhomogeneous broadening can be observed only for $\sigma/\delta > 0.2$.

3. Polymer dynamics

The donor decay can be written as [17–21]

$$p_{\text{dif}}(t) = 4\pi \int_0^\infty r^2 g_{\text{N}}(r, t) dr, \quad (28)$$

where the end-to-end distribution function for excited pairs, $g_{\text{N}}(r, t)$, is a function of time. For

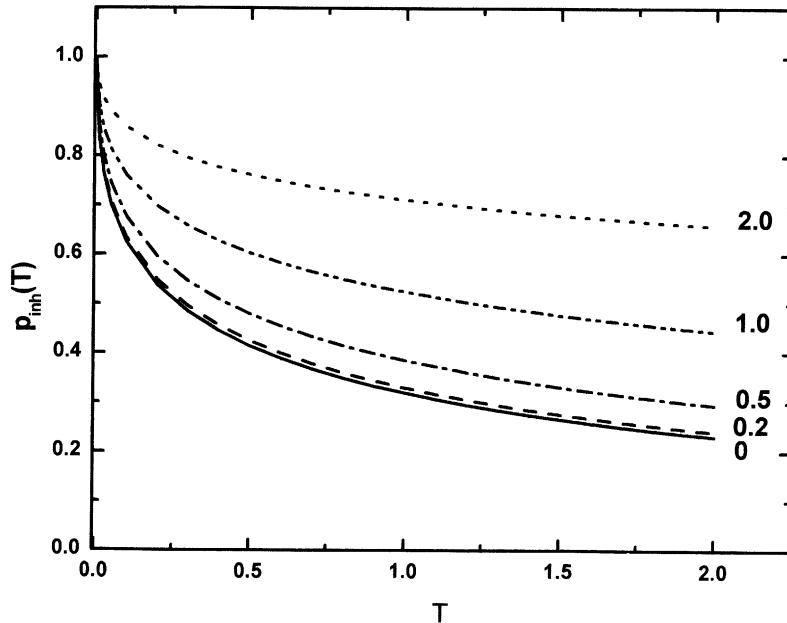


Fig. 4. Donor decay curve, $p(T)$ for a pseudo-ideal polymer chain considering the inhomogeneous spectra broadening, calculated from Eq. (26). The maximum of the fluorescence spectrum of the donor and the maximum of absorption spectra of the acceptor are at the same transition energy ($E_D = E_A$). The curves are labeled with the ratios between the inhomogeneous (σ) and homogeneous (δ) widths of spectral broadening.

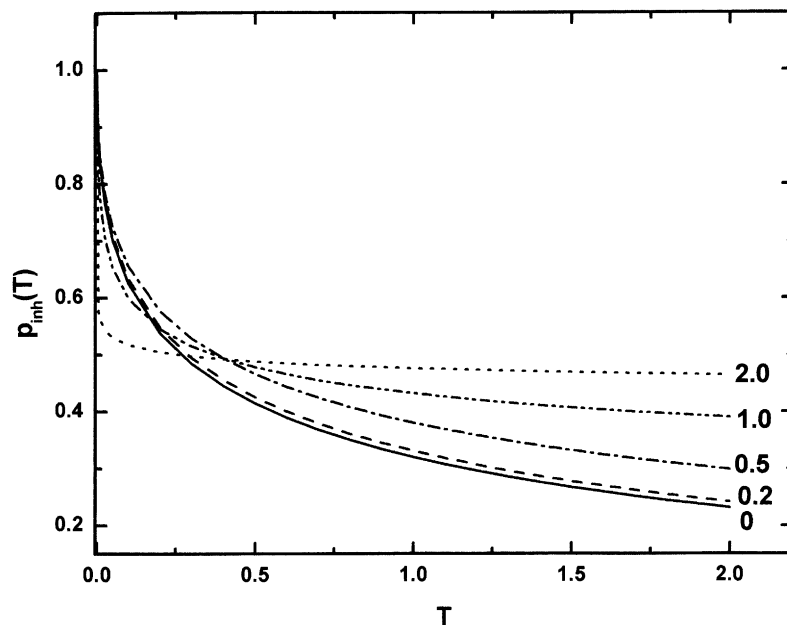


Fig. 5. Donor decay curve, $p(T)$, for a pseudo-ideal polymer chain considering the inhomogeneous spectra broadening, calculated from Eq. (26). The maximum of the fluorescence spectrum of the donor (E_D) and the maximum of absorption spectra of the acceptor (E_A) are at different transition energies ($E_D = E_A + 2\sigma$). The curves are labeled with the ratios between the inhomogeneous (σ) and homogeneous (δ) widths of spectral broadening.

$t = 0$, $g_N(r, t = 0) = g_N(r)$. For longer times, this is no longer the case, owing to two different factors: (i) preferential depletion of the pairs at short distances, owing to faster transfer; (ii) chain motion, owing to diffusion, counteracting depletion by energy transfer. This second factor is of course the more important the longer the lifetime of the donor, and the more fluid the solvent. When diffusion is fast enough to compensate for depletion by energy transfer, $g_N(r, t) \simeq g_N(r)$ for all times and the decay becomes single exponential (fast diffusion limit). When the diffusion is negligible, the results of Section 2.1 are retrieved. We will deal here with the situation intermediate between the two extreme cases mentioned.

The most appropriate chain model is the bead-spring model of Rouse [22] and Zimm [23]. The polymer chain is modeled as a system of n beads and $n-1$ entropic harmonic springs, being the mass concentrated in the beads that move in solution with friction coefficient, ζ . The Zimm model considers the hydrodynamic interactions, resulting from the coupling, mediated by the solvent, between the flow fields in different beads, which were disregarded in the primitive Rouse model. Both models predict a spectrum of relaxation times characteristic of large scale as well as short scale diffusive motions. In our case only the large scale diffusive motions are relevant, which simplify the problem. In this case the very simple harmonic spring model (two beads connected by a spring) can be used to describe the dynamics. When the distance between chromophores attached at the polymer chain ends change by small steps compared to R_0 , the distribution function, $g_N(r, t)$ obeys the diffusion equation [17,18],

$$\begin{aligned} \frac{\partial}{\partial t} g_N(r, t) = & D \frac{1}{r^2} \frac{\partial}{\partial r} r^2 \frac{\partial}{\partial r} g_N(r, t) \\ & + D \frac{1}{r^2} \frac{\partial}{\partial r} \left(r^2 g_N(r, t) \frac{\partial V}{\partial r} \right) \\ & - w(r) g_N(r, t), \end{aligned} \quad (29)$$

where D is the diffusion coefficient of the chain, and

$$V(r) = U(r)/kT = -\ln g_N(r). \quad (30)$$

$U(r)$ is a pseudo-potential of interaction between the beads, k is the Boltzmann constant and T the absolute temperature.

To obtain the time evolution of the distribution function the diffusion equation must be solved with appropriate boundary and initial conditions

$$\frac{\partial}{\partial r} g_N(r, t) + \frac{\partial}{\partial r} V(r)|_{r=r_0} = 0, \quad (31a)$$

$$g_N(r, 0) = g_N(r), \quad (31b)$$

where r_0 is the distance of closest approach.

The first two terms on the right-hand side of Eq. (29) describe the change of the distribution function $g_N(r, t)$ due to Brownian motion in the spherical potential $U(r)$, while the third one takes into account the decrease of the number of conformations due to the energy transfer events. The reflecting boundary condition ensures that the chromophores at both chain ends cannot approach closer than the distance r_0 .

Eq. (29) was solved numerically for a short polymer chains (N between 4 and 22) and chain end-to-end distribution function for both SAW chains [17,20,21] and pseudo-ideal polymer chains [18,19].

Introducing the dimensionless variables:

$$x = \frac{r}{\sqrt{\langle R_N^2 \rangle}}, \quad (32a)$$

$$D_r = \frac{D\tau \langle R_N^2 \rangle^2}{R_0^6} \quad (32b)$$

and the new function, $f(x, T)$

$$g_N(x, T) = f(x, T) g_N(x). \quad (32c)$$

Eq. (29) can be rewritten as

$$\frac{\partial}{\partial T} f(x, T) = D_r \frac{\partial^2}{\partial x^2} f + D_r \frac{\partial}{\partial x} f \left(\frac{2}{x} - \frac{\partial V}{\partial x} \right) - \frac{1}{x^6} f \quad (33)$$

with the initial and boundary conditions

$$f(x, 0) = 1, \quad (34a)$$

$$\frac{\partial}{\partial x} f(x, T)|_{x=x_0} = 0. \quad (34b)$$

The normalized potential, $V(x)$ obey the equation

$$\frac{\partial V}{\partial x} = 3x \quad (35)$$

as expected since the chain harmonic spring model was used. The donor decay curve is given by

$$p_{\text{dif}}(t) = 4\pi \int_0^\infty x^2 f(x, t) g_N(x) dx. \quad (36)$$

Fig. 6 shows the donor decay from Eq. (36) after performing the numerical integration of Eq. (33) with $x_0 = r_0 / \sqrt{\langle R_N^2 \rangle} = 0.01$ and boundary conditions given by Eq. (34a) and (34b). The results show that diffusion becomes important for values of the reduced diffusion coefficient, $D_r = D\tau \langle R_N^2 \rangle^2 / R_0^6 > 10^{-5}$.

For sufficiently long times the decay is exponential

$$p_{\text{dif}}(t) = \exp(-k_{\text{dif}} t) \quad (37)$$

with a rate constant given by (rapid diffusion limit)

$$k_{\text{dif}} = \frac{1}{\tau} 4\pi \int_{r_0}^\infty \left(\frac{R_0}{r}\right)^6 g_N(r) r^2 dr. \quad (38)$$

To obtain analytical results from this equation the distribution function $g_N(r)$, was approached by a rectangular function with width equal to $\sqrt{\langle R_N^2 \rangle}$ and $r_0 \ll \sqrt{\langle R_N^2 \rangle}$. For an ideal polymer chain (see Eq. (5)), we obtain

$$k_{\text{dif}}^{\text{id}} \cong \frac{1}{\tau} \frac{R_0^6}{\langle R_N^2 \rangle^{3/2} r_0^3}, \quad (39)$$

while for a SAW polymer chain (see Eq. (6)),

$$k_{\text{dif}}^{\text{SAW}} \cong \frac{1}{\tau} \frac{R_0^6}{\langle R_N^2 \rangle^{(3+5/18)/2} r_0^{3-5/18}}. \quad (40)$$

The differences between $k_{\text{dif}}^{\text{id}}$ and $k_{\text{dif}}^{\text{SAW}}$ are very small, owing to the small differences on the distribution function, $g_N(r)$, for θ and good solvents.

4. Conclusions

The energy transfer between chromophores attached to the ends of an isolated polymer chain

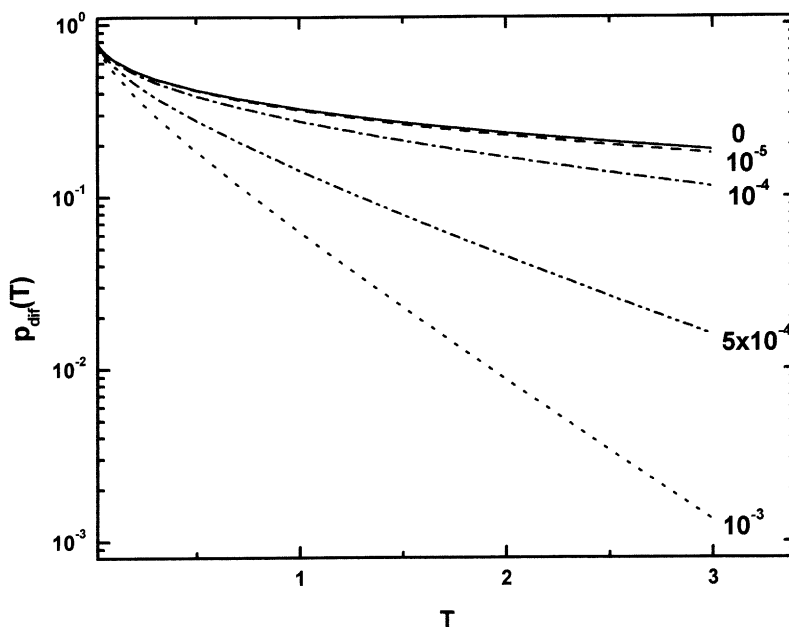


Fig. 6. Fluorescence donor decay curves, $p_{\text{dif}}(t)$, calculated from Eq. (36), for a pseudo-ideal polymer chain, considering the variation of end-to-end separation distance during the energy transfer time. The curves are labeled with the reduced diffusion coefficient, $D_r = D\tau \langle R_N^2 \rangle^2 / R_0^6$.

was studied. Chains labeled at both ends with different or identical fluorophores were considered. Interpolated analytical expressions were derived for the fluorescence decay curves taking into account the distribution of end-to-end separations in both θ and good solvents for the polymer. The donor decay curves for chains with dissimilar chromophores were compared with the exact solution obtained by numerical integration. The derived expressions depend on a single parameter, T , and reproduce the decay for all times with a precision better than 1% for pseudo-ideal chains and 3% for chains in good solvents.

The inhomogeneous broadening of chromophore spectra influences the decay curves for widths of inhomogeneous broadening, $\sigma > 0.2\delta$, where δ is the width of homogeneous broadening.

The effect of chain dynamics was described by a diffusion equation considering the chain harmonic spring model. Chain dynamics are important for values of the reduced diffusion coefficient, $D_r = D\tau\langle R_N^2 \rangle^2 / R_0^6 \geq 10^{-5}$, which implies donor fluorophores with long lifetimes, polymer chains with large diffusion coefficients and end-to-end separations, and fluorophores with small Förster energy transfer radius.

Acknowledgements

This work was supported by FCT. E.N.B. acknowledges an INVOTAN fellowship (ICCTI, Portugal).

References

- [1] S.E. Webber, Chem. Rev. 90 (1990) 1469.
- [2] B. Mollay, H.F. Kauffmann, in: R. Richert, A. Blumen (Eds.), Disorder Effects on Relaxation Processes, Springer, Berlin, 1994.
- [3] Th. Förster, Ann. Phys. 2 (1948) 55.
- [4] A.H. Marcus, D.M. Hussey, N.A. Diachun, M.D. Fayer, J. Chem. Phys. 103 (1995) 8189.
- [5] A.K. Roy, A. Blumen, J. Chem. Phys. 91 (1989) 4353.
- [6] G.H. Fredrickson, H.C. Andersen, C.W. Frank, J. Chem. Phys. 79 (1983) 3572.
- [7] M.D. Ediger, M.D. Fayer, Macromolecules 16 (1983) 1839.
- [8] K.A. Petersen, M.D. Fayer, J. Chem. Phys. 85 (1986) 4702.
- [9] K.A. Petersen, A.D. Stein, M.D. Fayer, Macromolecules 23 (1990) 111.
- [10] G.H. Fredrickson, H.C. Andersen, C.W. Frank, J. Polym. Sci.: Polym. Phys. Ed. 23 (1985) 591.
- [11] G.H. Fredrickson, H.C. Andersen, C.W. Frank, Macromolecules 16 (1983) 1456.
- [12] R.M. Pearlstein, J. Chem. Phys. 56 (1972) 2431.
- [13] P.D. Fitzgibbon, C.W. Frank, Macromolecules 15 (1982) 733.
- [14] G.H. Fredrickson, C.W. Frank, Macromolecules 16 (1983) 572.
- [15] A.Yu. Grosberg, A.R. Khokhlov, Statistical Physics of Macromolecules, AIP Press, New York, 1994.
- [16] M.N. Berberan-Santos, B. Valeur, J. Chem. Phys. 95 (1991) 8048.
- [17] E. Haas, E. Katchalski-Katzir, I.Z. Steinberg, Biopolymers 17 (1978) 11.
- [18] G. Liu, J.E. Guillet, Macromolecules 23 (1990) 2969.
- [19] G. Liu, J.E. Guillet, Macromolecules 23 (1990) 2973.
- [20] J.R. Lakowicz, J. Kusba, W. Wiczak, I. Gryczynski, M.L. Johnson, Chem. Phys. Lett. 173 (1990) 319.
- [21] J.R. Lakowicz, J. Kusba, I. Gryczynski, W. Wiczak, H. Szmajdzinski, M.L. Johnson, J. Phys. Chem. 95 (1991) 9654.
- [22] P.E. Rouse, J. Chem. Phys. 21 (1953) 1272.
- [23] B.H. Zimm, J. Chem. Phys. 24 (1956) 269.